*Research Report 110*

MAY 1964

# Reflection and Transmission Coefficients at the Interface Ice-Solid

by Hans Roethlisberger

U.S. ARMY MATERIEL COMMAND
COLD REGIONS RESEARCH & ENGINEERING LABORATORY
HANOVER, NEW HAMPSHIRE

## PREFACE

This is one of a series of reports of work accomplished on USA SIPRE* Project 022.01.034, Elastic and visco-elastic properties of snow and ice.

In this report, theoretical curves are presented which give the energy ratio of elastic plane waves reflected or refracted at an ideal plane interface between ice and a solid with the physical properties of soil or rock. Calculations were obtained by the digital computer.

The computer program was made by Dr. Roethlisberger, contract geophysicist, assisted by Ronald M. Van Noy†, who carried out most of the computations. Most of the plotting was done by Thomas J. Long†.

Work on this project was performed for the Basic Research Branch, Mr. J. A. Bender, then Branch Chief.

This report has been reviewed and approved for publication by Headquarters, U. S. Army Materiel Command.

W. L. NUNGESSER
Colonel, CE
Commanding
USA CRREL

Manuscript received 16 January 1962

DA Task 8X99-27-001-03

* Now redesignated U. S. Army Cold Regions Research and Engineering Laboratory

† At the time with U. S. Army Engineer Research and Development Detachment

## CONTENTS



## ILLUSTRATIONS



## TABLES

## SUMMARY

Nafe's (1957) presentation of reflection and transmission coefficients at a solid-solid interface was used to compute tables for the case of ice in contact with another solid at a plane interface. Energy ratios of all the combinations of reflected and refracted plane P and S waves were computed for 30 different cases of the second solid. A compressional velocity of 3.6 km/sec, a density of 0.9 g/cm$^3$, and a value of $\frac{1}{3}$ for Poisson's ratio were assumed for the ice. For the other solid, the velocity ranged from 1.2 to 6.0 km/sec, the density from 1.5 to 3.0 g/cm$^3$, and Poisson's ratio from 0 to $\frac{1}{3}$.

The computations were carried out with an electronic computer, and the results are presented graphically.

# REFLECTION AND TRANSMISSION COEFFICIENTS AT THE INTERFACE ICE-SOLID

by

Hans Roethlisberger

## INTRODUCTION

Nafe* has developed equations which are well suited for numerical computation of the fraction of the energy in a plane elastic wave incident upon a plane interface that is carried away in each of the reflected and refracted waves (reflection and refraction coefficients), and he has given tables and graphs for special cases of high velocity contrast. In most of his graphs, a highly complicated change of coefficients with the angle of emergence is noticed and the coefficients change by large amounts. This fact should have some significance in the seismic reflection method, if the angle of emergence deviates significantly from 90 degrees. Since a wide angle reflection technique has proven most effective for reflection soundings on shallow glaciers, it was felt that there is a need for the reflection coefficients at the interface of ice and other materials which occur at the bottom of glaciers.

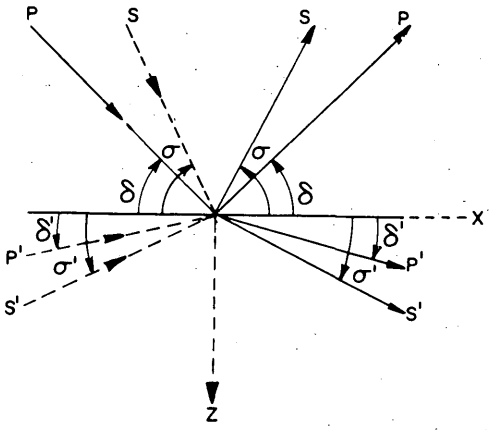


Figure 1. Notation.

In order to fill this need, a computer program was developed which produces a complete table of reflection and transmission coefficients for any combination of solids for angles of emergence from 90 to 0 degrees at any desired increment. Nafe's equations were used without modification and there is no need to repeat his presentation. Tables were computed with a Bendix G-15D electronic computer for the combination of ice with a variety of materials which represent the major groups of rocks and compacted frozen or unfrozen soils likely to occur under glaciers. The results are given in graphs. For identical density and velocity ratios, the same tables would apply to other materials than ice in contact with a second solid.

## DEFINITIONS

The same notation as used by Nafe is applied in the present report. He defines it in the following way (p. 205): "The notation employed is illustrated in Figure 1. All quantities referring to the lower medium are primed and those referring to the upper medium are unprimed. The angle $\sigma$ specifies the angle of emergence (complement of angle of incidence) for an S wave, and $\delta$ that for a compressional wave. (Only SV is considered here and SV will be shortened to S.) Each of the four possible incident waves shown in Figure 1 will give rise to a set of four outgoing waves having only the directions specified in the diagram. The amplitudes will be written, for example, (PS') or (P'P) where the outgoing wave is written first and the incident wave second."

The energy ratio of emergent wave X to incident wave Y, i.e., the fraction of energy incident in Y that is carried by X, is written E(X Y), for example E(P S') or E(P' P). It can be shown that E(X Y) is equal to E(Y X).

## COMPUTATION

One computer program was designed to produce the tables, additional ones were found to be necessary for the critical angles and certain checks.

---

* Nafe, J. E. (1957) Reflection and transmission coefficients at a solid-solid interface of high velocity contrast, Bulletin of the Seismological Society of America, vol. 47, no. 3, p. 205-219.

The main program was written in Intercom 1000 single-precision, a programming system for the Bendix G-15D computer permitting input and output with five significant digits. However, only three digits were printed after the decimal point in the tables, using fixed-point output. The figures were truncated at the last digit, i.e., not rounded out. The main program used almost the complete storage space of the computer, and an extra single-precision program was used to compute critical angles and corresponding energy ratios.

It was found that under certain critical conditions, when differences of almost equal quantities occur in the equation, the results become inaccurate. This is true for the velocity ratio of 1 for very small angles. In order to check the tables, the energy ratios for a large number of individual angles of emergence were computed with a double-precision program which gives twelve significant digits. Only a very few small differences in the last digit were found between the double and single-precision computation, and it is believed that the latter is correct to better than two digits for all the angles used in the tables.

Table I is an example of the results as they are typed out by the computer. The first line at the head of the table gives the densities $\rho$ and $\rho'$, compressional velocities $a$ and $a'$, shear velocities $\beta$ and $\beta'$ and Poisson's ratios $\nu$ and $\nu'$ of the upper and lower medium respectively. In the second line, the density and velocity ratios are given. These are dimensionless and are the true parameters of the table. The first part of the table gives the reflection and transmission coefficients of the various wave combinations for angles of emergence of the compressional wave in the upper medium $\delta$, which changes from line to line by steps of 2 degrees. The second part of the table gives the coefficients for the argument $\sigma'$ for the waves which remain beyond their critical angle at $\delta = 0$. At the bottom of the table, coefficients are given for the critical angle $\delta_{crit}$ as the argument.

The second part of the table only exists when the shear velocity of the lower medium is less than the compressional velocity of the upper one. The computer program was written to make all the necessary decisions automatically on whether or not a second table exists and which columns to break off beyond the critical angle in the first part of the table.

For angles beyond critical, certain terms of the amplitude equations become complex. In the expressions for the energy ratios, the product of complex terms and the complex conjugates occurs. In the computer program, two storage locations were assigned to each expression which could be either real or imaginary, and the numerical value of the expression was stored in the proper location depending on the case; zero was stored in the alternative location. Later steps in the computation were then carried out with the contents of both storage locations, and consecutive storage was handled in the same way. When the product of the final complex term and the complex conjugate was formed, the real and imaginary parts were combined, since the product is equal to the sum of the squares of the two parts. The operation also worked if one of the parts was zero, i.e., for purely real or imaginary amplitude expressions. This approach had the advantage that one single program handled all possible cases. Otherwise different program sections would have been necessary for angles below or above critical. The latter method would have given faster computation, but might have used up more storage space for the program; this was not investigated, however. The program used filled almost all the available storage space of the computer.

The program was designed to produce tables acceptable for reproduction. Nevertheless, preference was given to presenting the results in the form of graphs, since it was believed that graphs would give adequate accuracy and make it possible to condense the information to much smaller space. While in the tables the angles $\delta$ and $\sigma'$ were used as arguments, in the figures it was more appropriate to present some of the coefficients versus other angles. The necessary conversions were carried out with standard tables of trigonometric functions or by slide rule. In a number of cases, tables were produced for interchanged upper and lower media (i.e., for the arguments $\delta'$ and $\sigma$), which gave additional data for the graphs.

## RESULTS

For convenience, round figures were used for the properties of ice and the solids in contact with it. The properties for ice were compressional velocity $\alpha = 3.6$ km/sec, density $\rho = 0.9$ g/cm$^3$, shear velocity $\beta = 1.8$ km/sec corresponding with Poisson's ratio $\nu = \frac{1}{3}$. In Table II, the properties of the lower medium are given for the thirty cases which were computed. Absolute and dimensionless figures are both given, the latter ones referring to an upper medium with compressional velocity and density equal to 1 and Poisson's ratio of $\frac{1}{3}$. These ratios are given in recognition that the upper solid need not necessarily be ice, but any material with Poisson's ratio of $\frac{1}{3}$.

The results of the computation are plotted in Figures 2 to 11. Each figure gives the energy ratio of one combination of incident and emergent waves. There are 16 such combinations, but the number is reduced to 10 because of the equality of E(X Y) and E(Y X). Each figure contains six graphs which contain the 30 curves corresponding to the 30 different lower media listed in Table II. The groups are formed according to the compressional velocity in the lower medium so that each graph presents curves for one P'-velocity, but different densities and Poisson's ratios (shear velocities). For the compressional velocity, six different values were used, represented by the six groups of curves, while only three different values were chosen for both the density and Poisson's ratio. This would lead to nine combinations in each P' velocity group, but not all of them have been carried out. No high densities were used together with low velocities and vice versa (no low densities with high velocities), and often a choice of only two values for Poisson's ratio was applied instead of all three. Although the grouping according to compressional velocity is only appropriate in cases where one or both of the incident or emergent waves is a P-wave, it has not been changed in the cases of pure shear-wave combinations, in order to keep the same groups for all the figures. This is the reason why the P-wave combinations give more perspicuous figures, i.e., with less intersecting curves than the shear waves.

The curves given for the abscissa $\delta$ were obtained from points at every 2 degrees, plus those at critical angles, i.e., from a minimum of 46 points. In some of the cases where the energy ratios are plotted against other angles than $\delta$ or $\sigma'$, a smaller number of values were available from the tables due to the conversion of the angles, and the points have not been evenly spaced. In the cases where the interval between two computed values is too big to draw the curve accurately, dotted lines are used. The same technique is used in some cases when sharp maxima or minima appear in a 2-degree interval. If needed, it would be an easy task to produce additional values for smaller increments of $\delta$ and $\sigma'$ with the same computer program.

In most cases, there is a general trend in the curves of one graph and a certain change in trend from graph to graph. For many possible combinations of parameters, it is therefore possible to interpolate between curves in one graph, if intermediate values of density and Poisson's ratio are required, or between successive graphs if intermediate compressional velocity is involved. For interpolation between shear-wave combinations, it would be advantageous to rearrange the curves. Interpolation is least accurate, if not impossible, for the peak values at very sharp peaks for certain critical angles, and in the immediate neighborhood of the peaks.

Very rapid changes of the energy ratios and especially sharp narrow peaks are quite common. The most abrupt maxima and minima are found at the critical angle in the cases where the compressional velocities are the same in the upper and lower media, the peaks and troughs being one and zero, respectively, in this case. For the curves nos. 11, 13, and 16, where both the compressional and the shear wave velocity are the same in both media, the extremes of E(S S), for example, jump from almost 0 to 1 and back to almost 0.

For practical application, where the waves originate from a point source and plane waves are only an approximation, the sharp extremes of the curves probably have little significance. However, where the curves show a slow change with the angle of emergence, the results for plane waves as presented here should be applicable in practice.

There are significant differences between the curves for different materials under ice. This makes it likely that energy considerations could help to identify the nature of a reflector under a glacier with wide angle reflections. Disturbing effects of layering at the bottom of the ice (dirt bands) and deviations from a plane interface must be expected. Field experiments on shallow ice bodies over different rocks and soils would be of interest.

Table I. Reflection and transmission coefficients for two solids defined at the head of the table.

| | $\rho$ (g/cm$^3$) $\rho/\rho$ | $\rho'$ (g/cm$^3$) $\rho'/\rho$ | a (km/sec) a/a | a' (km/sec) a'/a | $\beta$ (km/sec) $\beta/a$ | $\beta'$ (km/sec) $\beta'/a$ | $\nu$ | $\nu'$ | | |
|---|---|---|---|---|---|---|---|---|---|---|
| | .900 | 3.000 | 3.600 | 4.800 | 1.800 | 2.771 | .333 | .250 | | |
| | 1.000 | 3.333 | 1.000 | 1.333 | .500 | .769 | .333 | .250 | | |
| $\delta$ | E(P P) | E(S S) | E(P'P') | E(S'S') | E(S P) | E(P'P) | E(S'P) | E(P'S) | E(S'S) | E(S'P') |
| 90.000 | .400 | .454 | .400 | .454 | .000 | .599 | .000 | .000 | .545 | .000 |
| 88.000 | .399 | .452 | .397 | .450 | .001 | .599 | .000 | .000 | .546 | .002 |
| 86.000 | .395 | .448 | .388 | .441 | .004 | .599 | .000 | .000 | .546 | .011 |
| 84.000 | .389 | .442 | .375 | .426 | .010 | .598 | .001 | .000 | .546 | .025 |
| 82.000 | .382 | .433 | .356 | .405 | .017 | .597 | .002 | .001 | .547 | .044 |
| 80.000 | .372 | .421 | .333 | .380 | .027 | .596 | .003 | .002 | .547 | .067 |
| 78.000 | .360 | .407 | .306 | .350 | .039 | .594 | .005 | .003 | .548 | .094 |
| 76.000 | .346 | .392 | .277 | .317 | .052 | .592 | .007 | .005 | .549 | .124 |
| 74.000 | .331 | .374 | .245 | .282 | .067 | .590 | .010 | .007 | .551 | .156 |
| 72.000 | .314 | .354 | .212 | .245 | .083 | .588 | .012 | .009 | .552 | .189 |
| 70.000 | .297 | .333 | .179 | .208 | .100 | .586 | .015 | .011 | .554 | .222 |
| 68.000 | .278 | .311 | .147 | .171 | .118 | .584 | .018 | .014 | .555 | .253 |
| 66.000 | .259 | .287 | .117 | .136 | .137 | .581 | .021 | .017 | .558 | .283 |
| 64.000 | .240 | .263 | .089 | .104 | .155 | .579 | .025 | .020 | .560 | .310 |
| 62.000 | .220 | .238 | .065 | .074 | .173 | .576 | .028 | .024 | .563 | .333 |
| 60.000 | .201 | .213 | .044 | .049 | .191 | .574 | .032 | .029 | .566 | .351 |
| 58.000 | .183 | .188 | .027 | .029 | .207 | .573 | .035 | .034 | .569 | .364 |
| 56.000 | .166 | .163 | .015 | .014 | .222 | .572 | .038 | .039 | .574 | .372 |
| 54.000 | .150 | .138 | .007 | .004 | .235 | .571 | .041 | .046 | .579 | .374 |
| 52.000 | .137 | .115 | .002 | .000 | .245 | .573 | .043 | .054 | .585 | .370 |
| 50.000 | .127 | .092 | .000 | .000 | .251 | .576 | .045 | .062 | .593 | .360 |
| 48.000 | .121 | .070 | .000 | .005 | .251 | .581 | .044 | .073 | .604 | .344 |
| 46.000 | .125 | .049 | .000 | .013 | .243 | .589 | .040 | .085 | .621 | .324 |
| 44.000 | .153 | .028 | .006 | .020 | .218 | .597 | .030 | .099 | .652 | .296 |
| 42.000 | .312 | .007 | .121 | .014 | .142 | .540 | .004 | .103 | .746 | .234 |
| 40.000 | .571 | .022 | | .108 | .257 | | .171 | | .720 | |
| 38.000 | .339 | .029 | | .192 | .411 | | .249 | | .558 | |
| 36.000 | .241 | .027 | | .237 | .484 | | .273 | | .488 | |
| 34.000 | .200 | .022 | | .264 | .521 | | .278 | | .456 | |
| 32.000 | .188 | .016 | | .281 | .538 | | .273 | | .444 | |
| 30.000 | .191 | .012 | | .292 | .544 | | .264 | | .443 | |
| 28.000 | .204 | .010 | | .298 | .541 | | .253 | | .447 | |
| 26.000 | .225 | .009 | | .302 | .533 | | .241 | | .456 | |
| 24.000 | .251 | .011 | | .304 | .520 | | .228 | | .467 | |
| 22.000 | .283 | .016 | | .304 | .502 | | .214 | | .481 | |
| 20.000 | .319 | .022 | | .302 | .480 | | .200 | | .496 | |
| 18.000 | .360 | .032 | | .300 | .453 | | .185 | | .513 | |
| 16.000 | .406 | .043 | | .296 | .423 | | .170 | | .532 | |
| 14.000 | .456 | .057 | | .292 | .388 | | .154 | | .553 | |
| 12.000 | .513 | .074 | | .287 | .349 | | .137 | | .575 | |
| 10.000 | .575 | .093 | | .280 | .305 | | .118 | | .600 | |
| 8.000 | .643 | .115 | | .273 | .257 | | .098 | | .627 | |
| 6.000 | .719 | .140 | | .265 | .202 | | .077 | | .656 | |
| 4.000 | .803 | .168 | | .256 | .142 | | .054 | | .689 | |
| 2.000 | .896 | .200 | | .246 | .074 | | .028 | | .724 | |
| .000 | 1.000 | .235 | | .235 | .000 | | .000 | | .764 | |

Table I. (Cont'd) Reflection and transmission coefficients for two solids defined at the head of the table.

| σ' | E(SS) | E(S'S') | E(S'S) |
|---|---|---|---|
| 38.000 | .330 | .330 | .669 |
| 36.000 | .400 | .400 | .599 |
| 34.000 | .458 | .458 | .541 |
| 32.000 | .508 | .508 | .491 |
| 30.000 | .550 | .550 | .449 |
| 28.000 | .588 | .588 | .411 |
| 26.000 | .621 | .621 | .378 |
| 24.000 | .650 | .650 | .349 |
| 22.000 | .677 | .677 | .322 |
| 20.000 | .702 | .702 | .297 |
| 18.000 | .726 | .726 | .273 |
| 16.000 | .749 | .749 | .250 |
| 14.000 | .773 | .773 | .226 |
| 12.000 | .798 | .798 | .201 |
| 10.000 | .825 | .825 | .174 |
| 8.000 | .854 | .854 | .145 |
| 6.000 | .886 | .886 | .113 |
| 4.000 | .921 | .921 | .078 |
| 2.000 | .959 | .959 | .040 |
| .000 | 1.000 | 1.000 | .000 |

| $\delta_{crit}$ | | | | | | | | | | |
|---|---|---|---|---|---|---|---|---|---|---|
| 41.409[a] | .929 | .000 | 1.000 | .000 | .035 | .000 | .035 | .000 | .964 | .000 |

a Critical angle for δ' = 0

Table II. Properties of lower medium.

| Curve no. | Compressional velocity $\alpha'$ (km/sec) | Density $\rho'$ (g/cm$^3$) | Poisson's ratio $\nu'$ | Shear velocity $\beta'$ (km/sec) | Compressional velocity ratio $\alpha'/\alpha$ | Density ratio $\rho'/\rho$ |
|---|---|---|---|---|---|---|
| 1 | 1.2 | 1.5 | 0 | .848 | .333 | 1.666 |
| 2 | 1.2 | 1.5 | 1/4 | .692 | .333 | 1.666 |
| 3 | 1.2 | 1.5 | 1/3 | .600 | .333 | 1.666 |
| 4 | 2.4 | 1.5 | 0 | 1.697 | .666 | 1.666 |
| 5 | 2.4 | 1.5 | 1/4 | 1.385 | .666 | 1.666 |
| 6 | 2.4 | 1.5 | 1/3 | 1.200 | .666 | 1.666 |
| 7 | 2.4 | 2.0 | 0 | 1.697 | .666 | 2.222 |
| 8 | 2.4 | 2.0 | 1/4 | 1.385 | .666 | 2.222 |
| 9 | 2.4 | 2.0 | 1/3 | 1.200 | .666 | 2.222 |
| 10 | 3.6 | 1.5 | 1/4 | 2.078 | 1.000 | 1.666 |
| 11 | 3.6 | 1.5 | 1/3 | 1.800 | 1.000 | 1.666 |
| 12 | 3.6 | 2.0 | 0 | 2.545 | 1.000 | 2.222 |
| 13 | 3.6 | 2.0 | 1/3 | 1.800 | 1.000 | 2.222 |
| 14 | 3.6 | 3.0 | 0 | 2.545 | 1.000 | 3.333 |
| 15 | 3.6 | 3.0 | 1/4 | 2.078 | 1.000 | 3.333 |
| 16 | 3.6 | 3.0 | 1/3 | 1.800 | 1.000 | 3.333 |
| 17 | 4.2 | 1.5 | 1/4 | 2.424 | 1.166 | 1.666 |
| 18 | 4.2 | 2.0 | 1/3 | 2.100 | 1.166 | 2.222 |
| 19 | 4.2 | 3.0 | 0 | 2.969 | 1.166 | 3.333 |
| 20 | 4.2 | 3.0 | 1/4 | 2.424 | 1.166 | 3.333 |
| 21 | 4.8 | 1.5 | 1/4 | 2.771 | 1.333 | 1.666 |
| 22 | 4.8 | 1.5 | 1/3 | 2.400 | 1.333 | 1.666 |
| 23 | 4.8 | 2.0 | 1/4 | 2.771 | 1.333 | 2.222 |
| 24 | 4.8 | 2.0 | 1/3 | 2.400 | 1.333 | 2.222 |
| 25 | 4.8 | 3.0 | 0 | 3.394 | 1.333 | 3.333 |
| 26 | 4.8 | 3.0 | 1/4 | 2.771 | 1.333 | 3.333 |
| 27 | 4.8 | 3.0 | 1/3 | 2.400 | 1.333 | 3.333 |
| 28 | 6.0 | 3.0 | 0 | 4.242 | 1.666 | 3.333 |
| 29 | 6.0 | 3.0 | 1/4 | 3.464 | 1.666 | 3.333 |
| 30 | 6.0 | 3.0 | 1/3 | 3.000 | 1.666 | 3.333 |

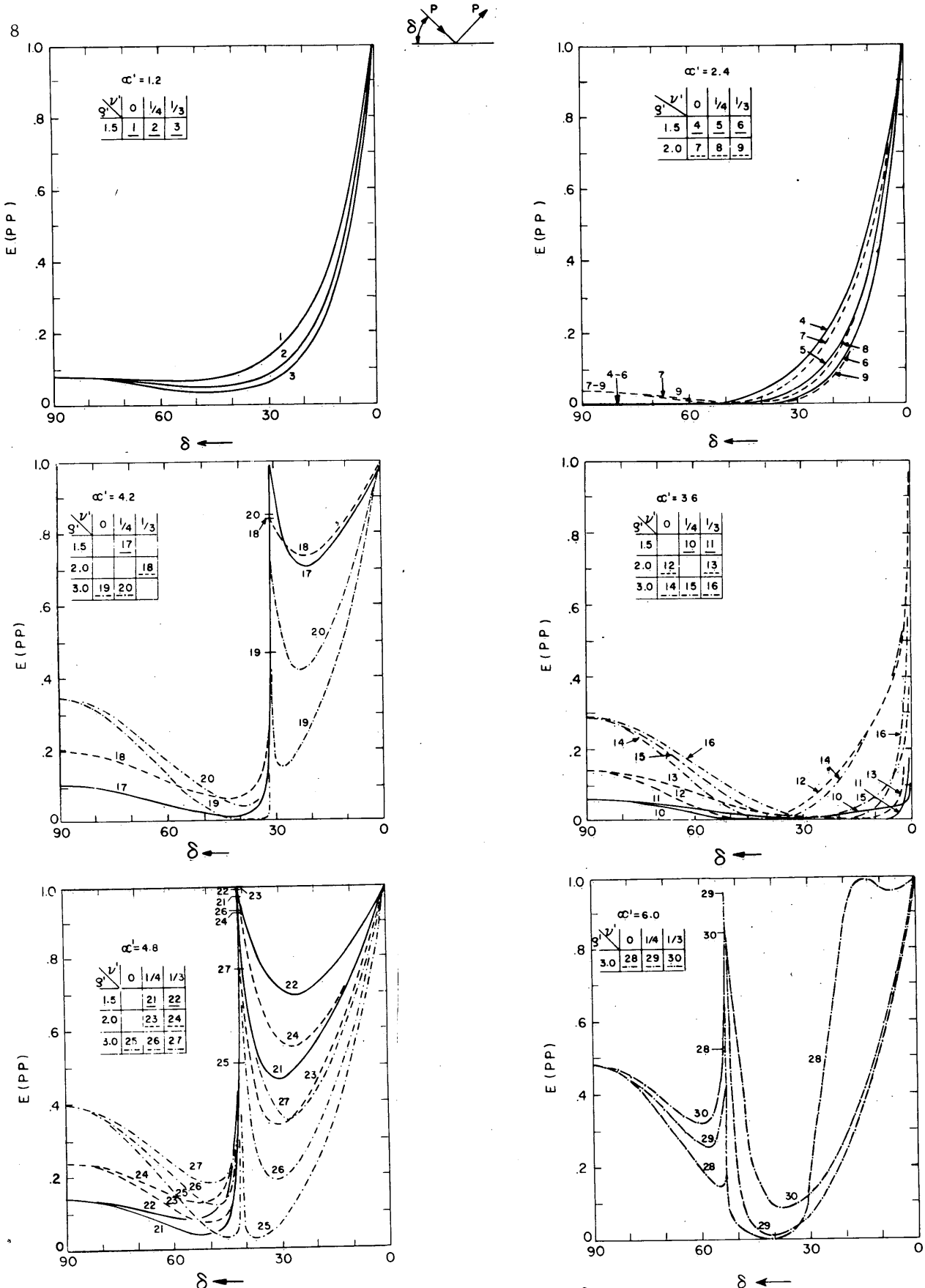


Figure 2. E (P P) vs δ

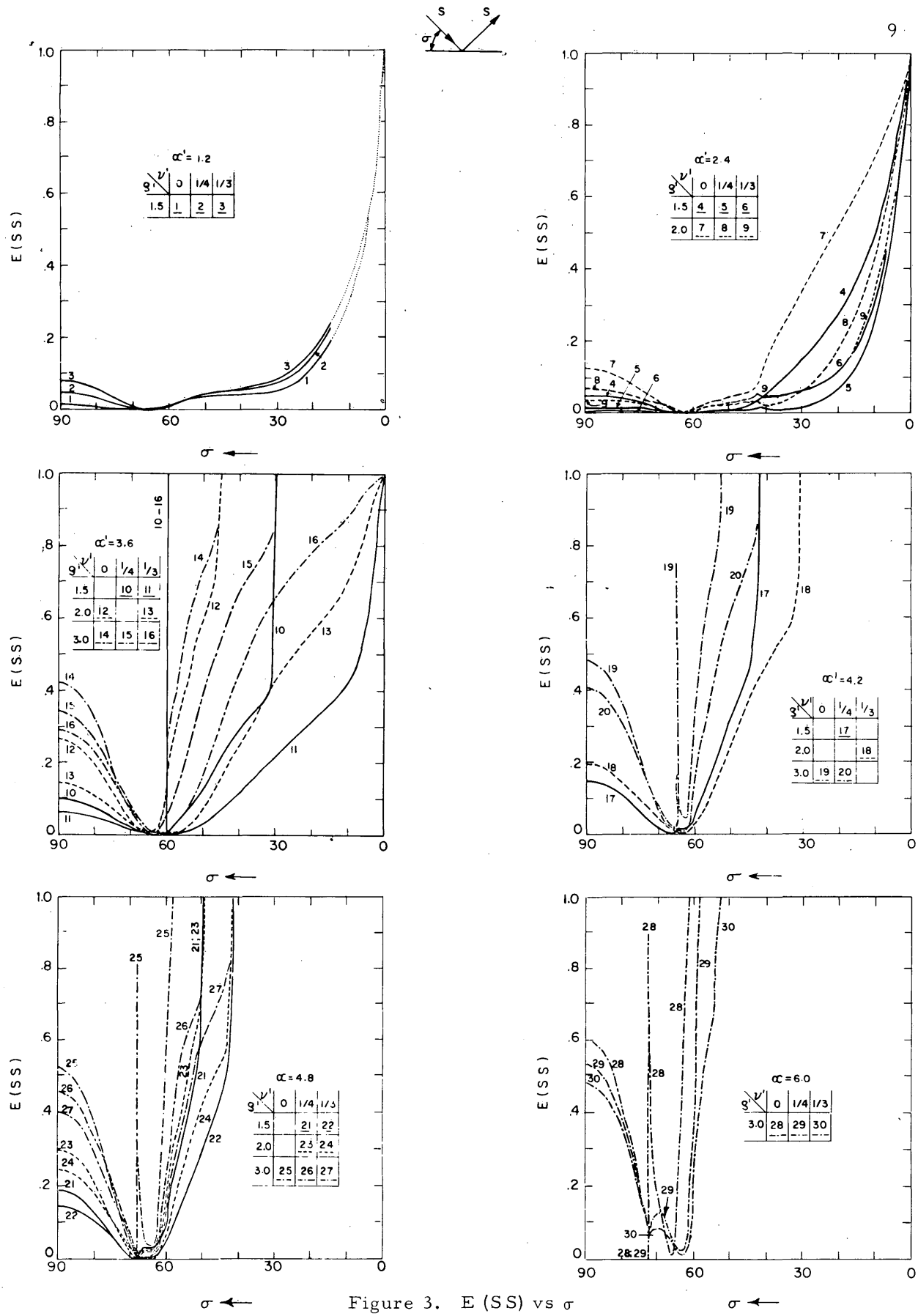


Figure 3. E (SS) vs σ

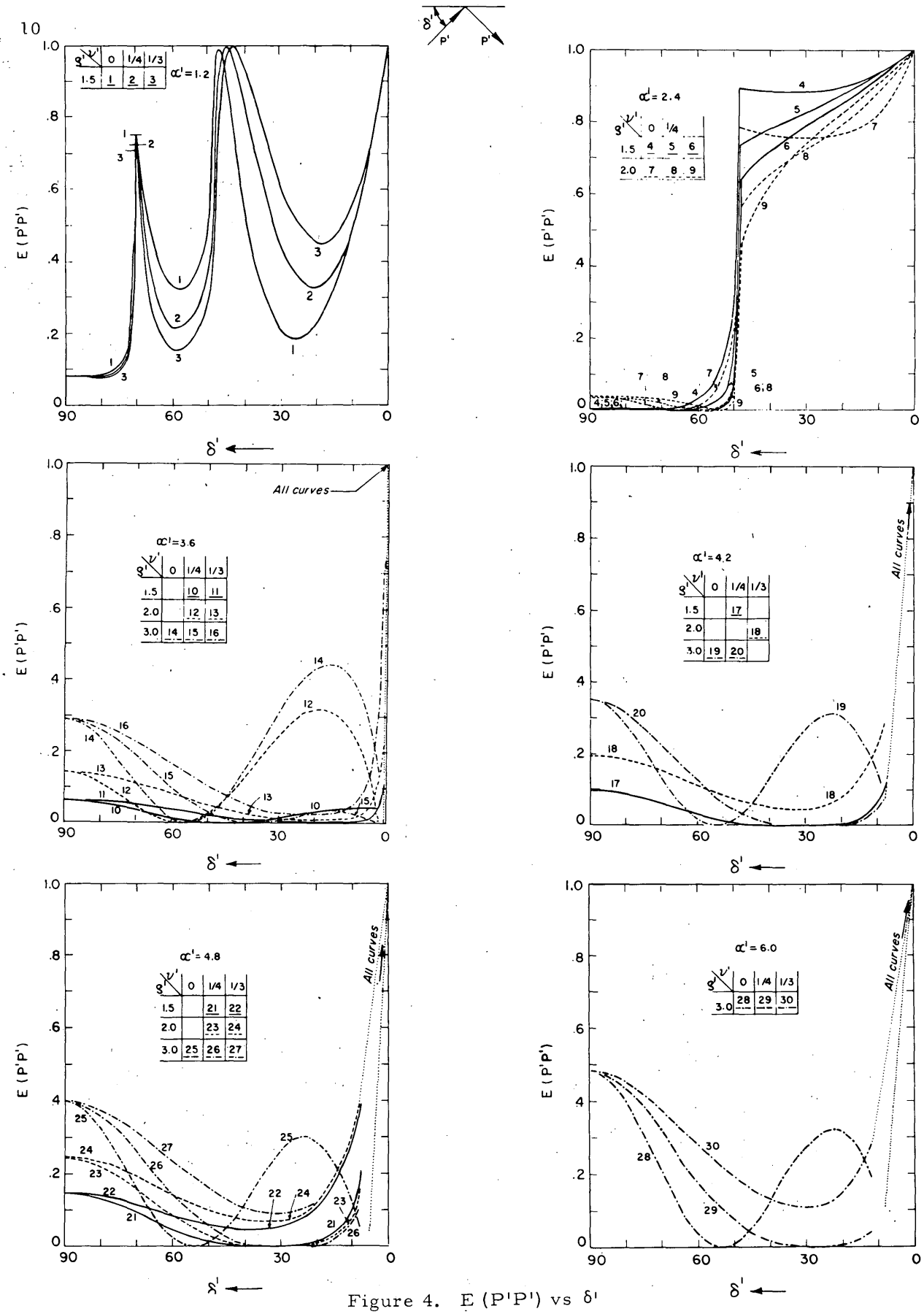


Figure 4. E (P'P') vs δ'

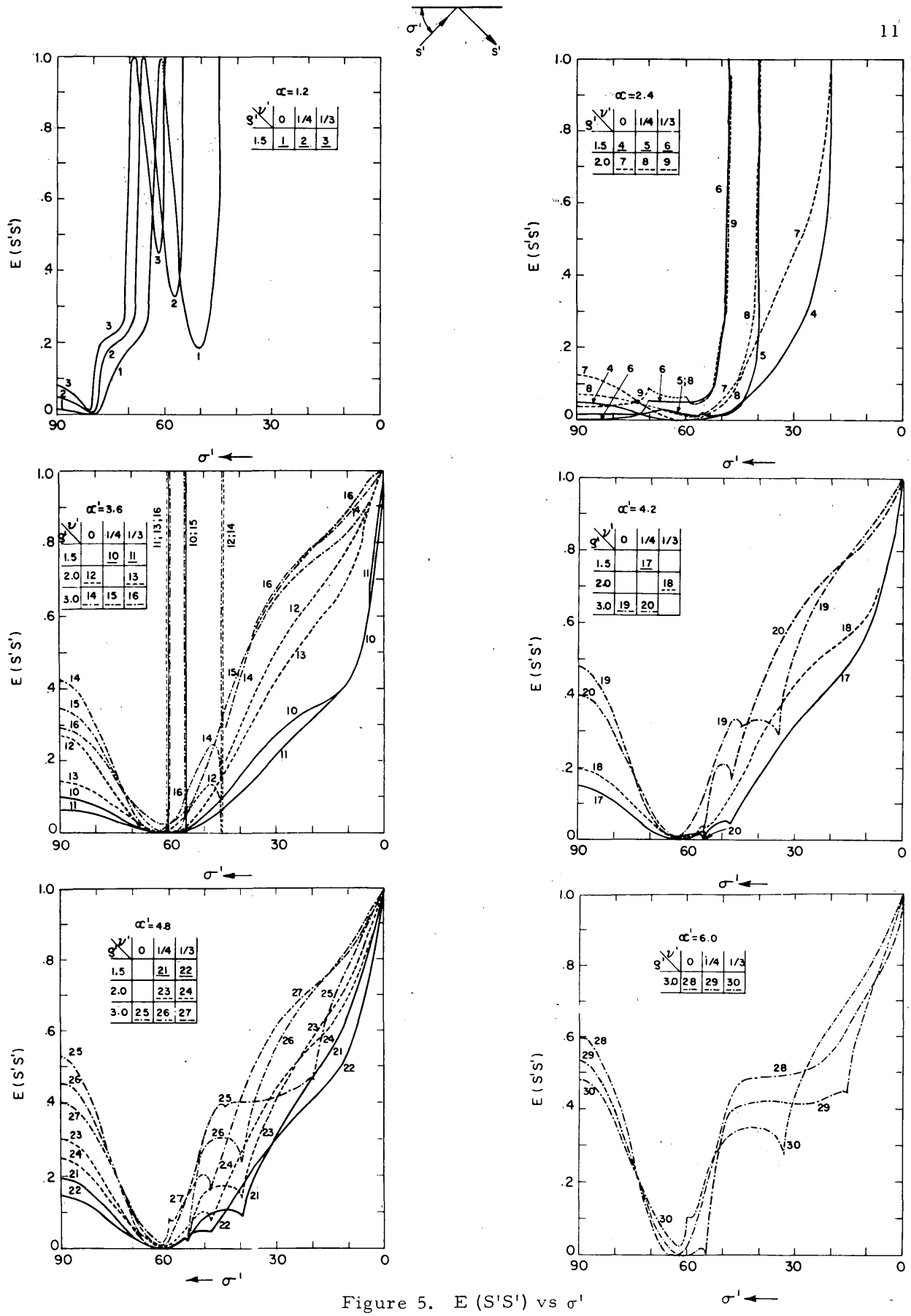


Figure 5. E (S'S') vs σ'

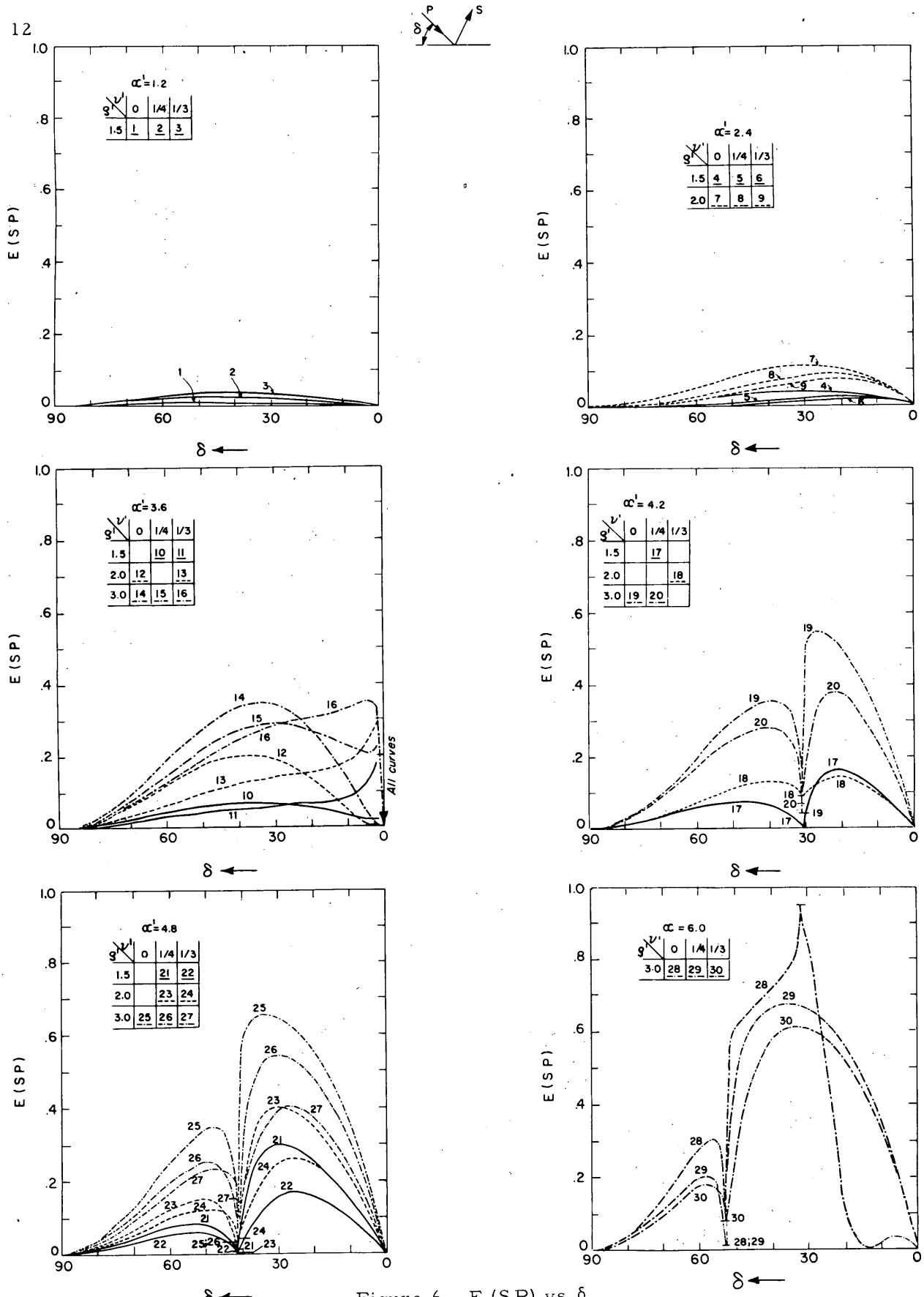


Figure 6. E (S P) vs δ

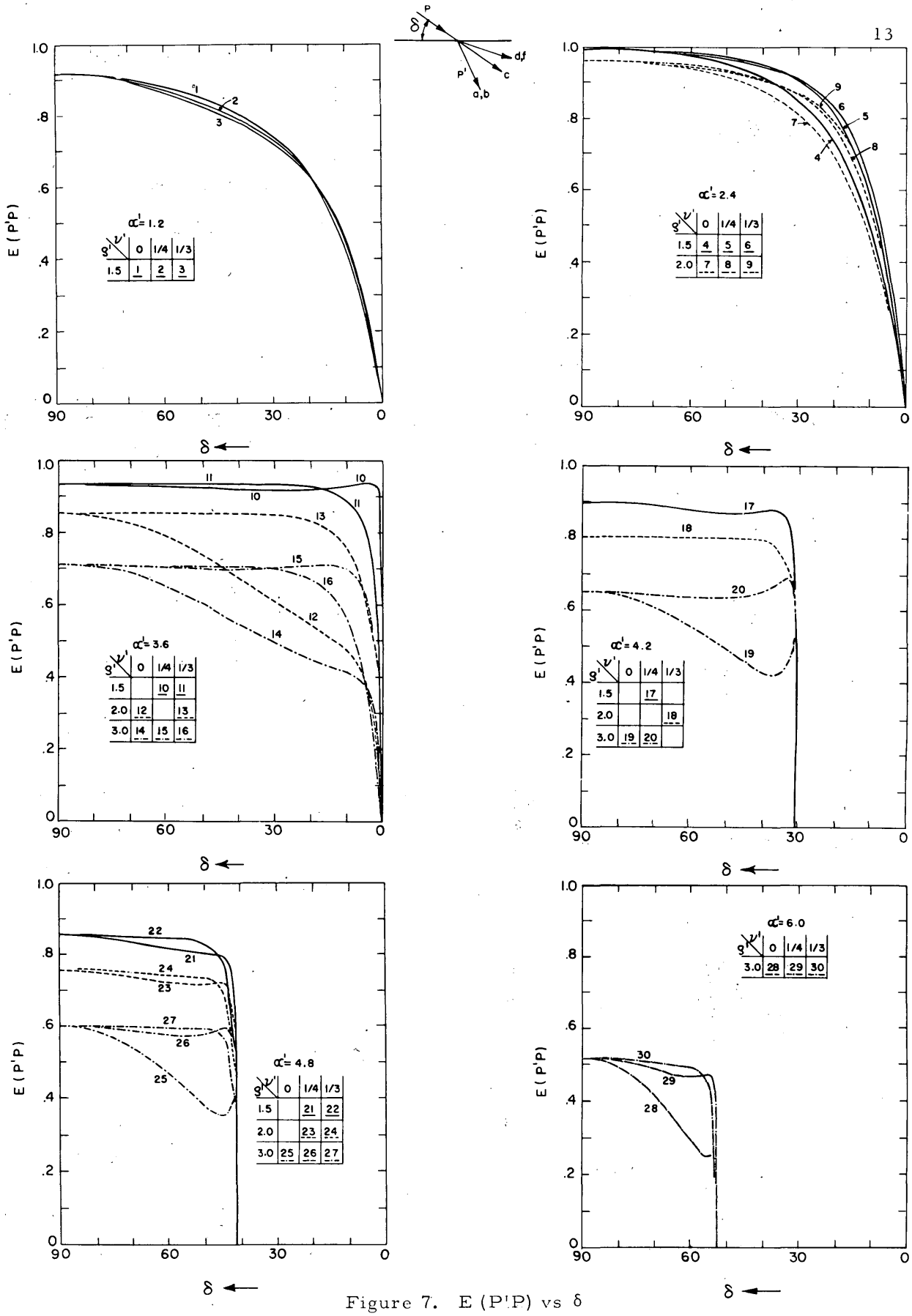


Figure 7. E (P'P) vs δ

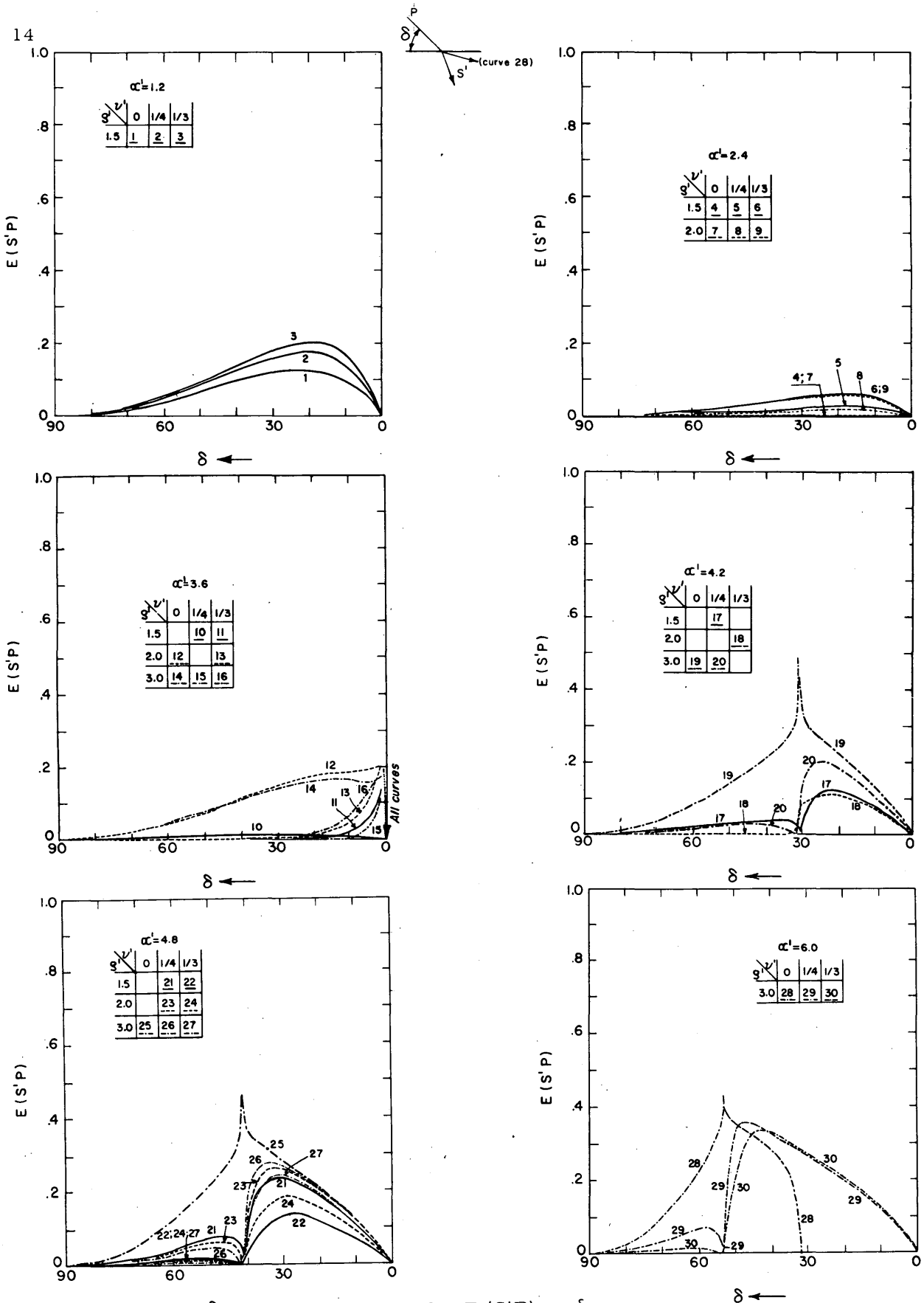


Figure 8. E (S'P) vs δ

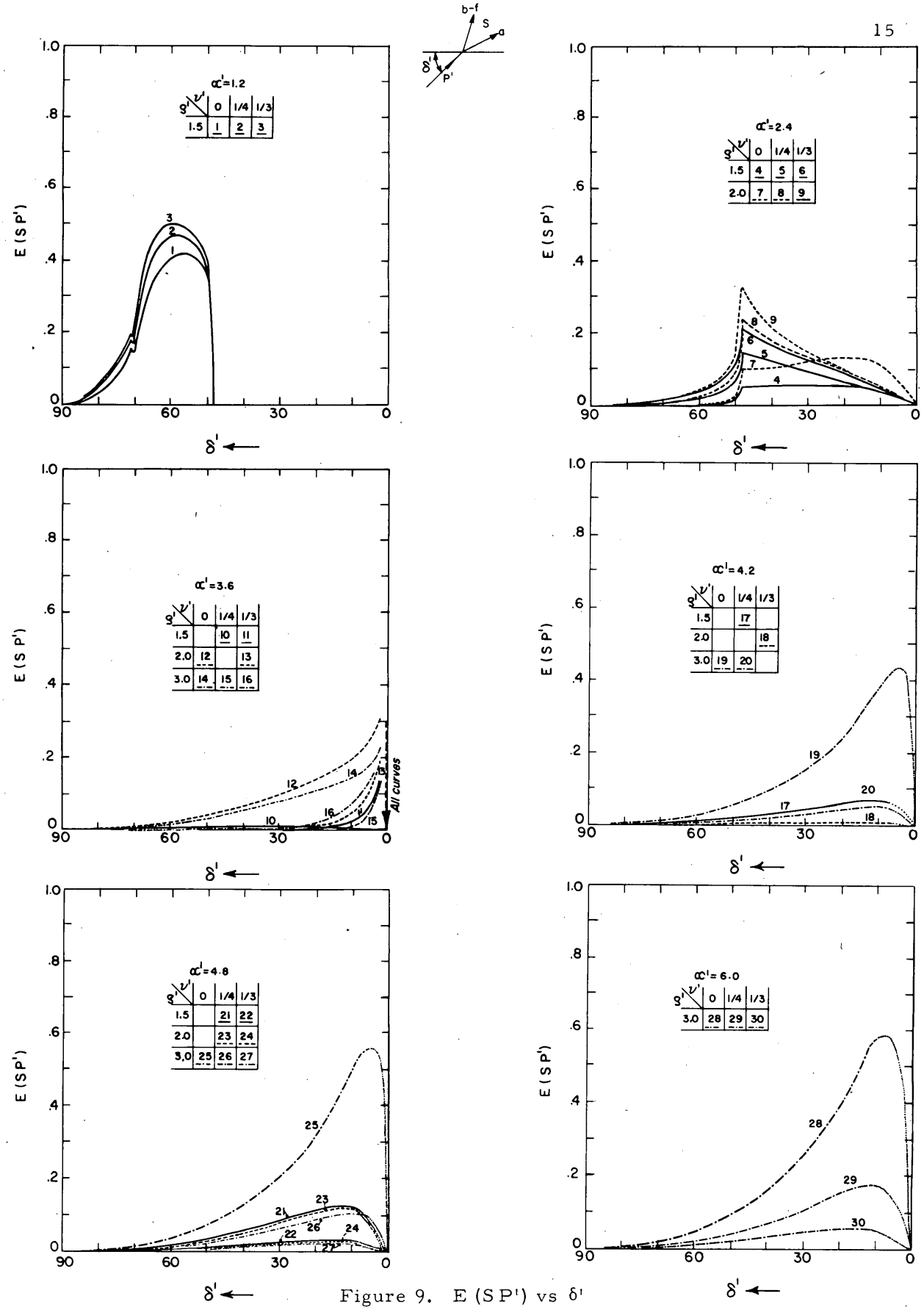


Figure 9. E (S P') vs δ'

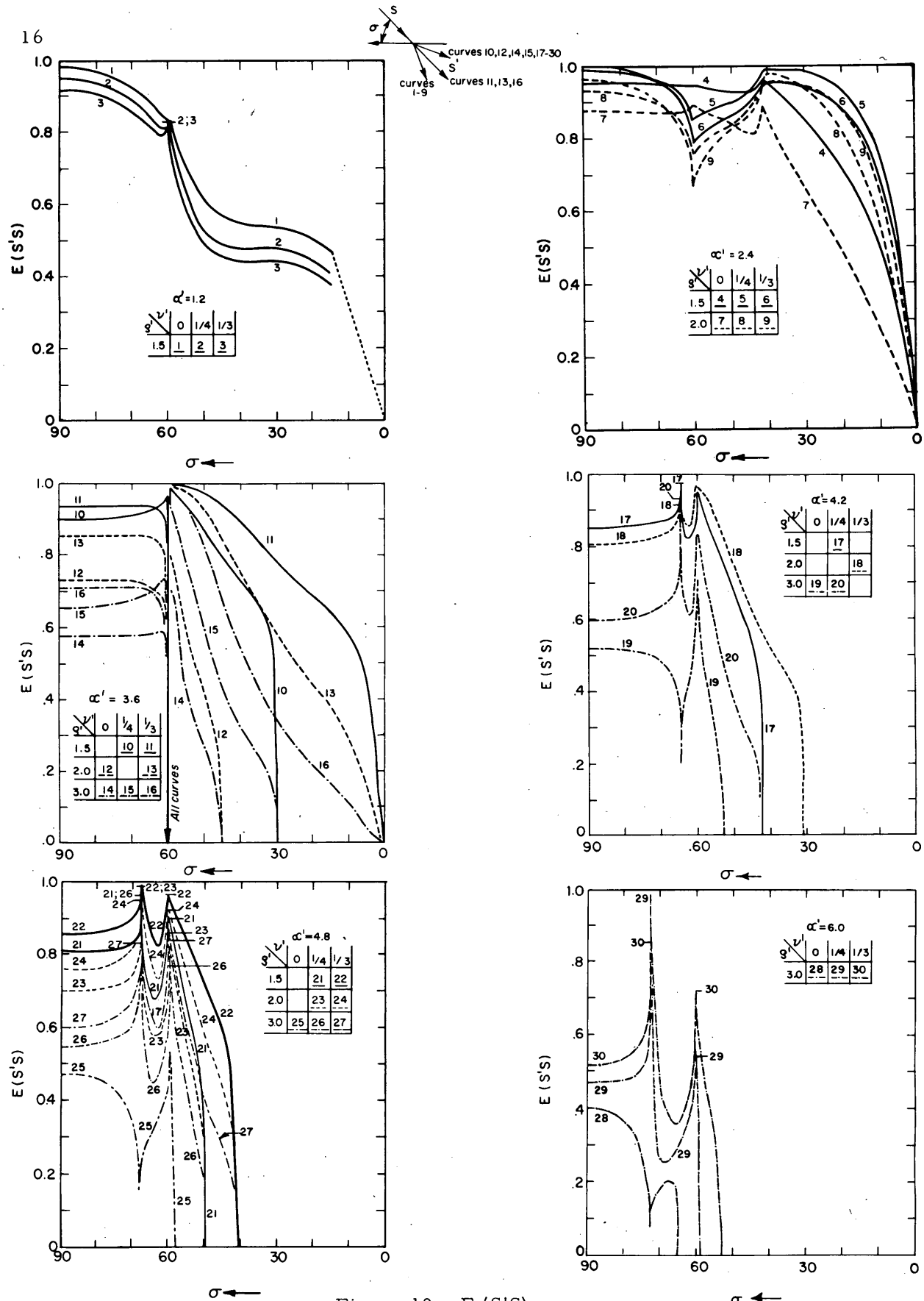


Figure 10. E (S'S) vs σ

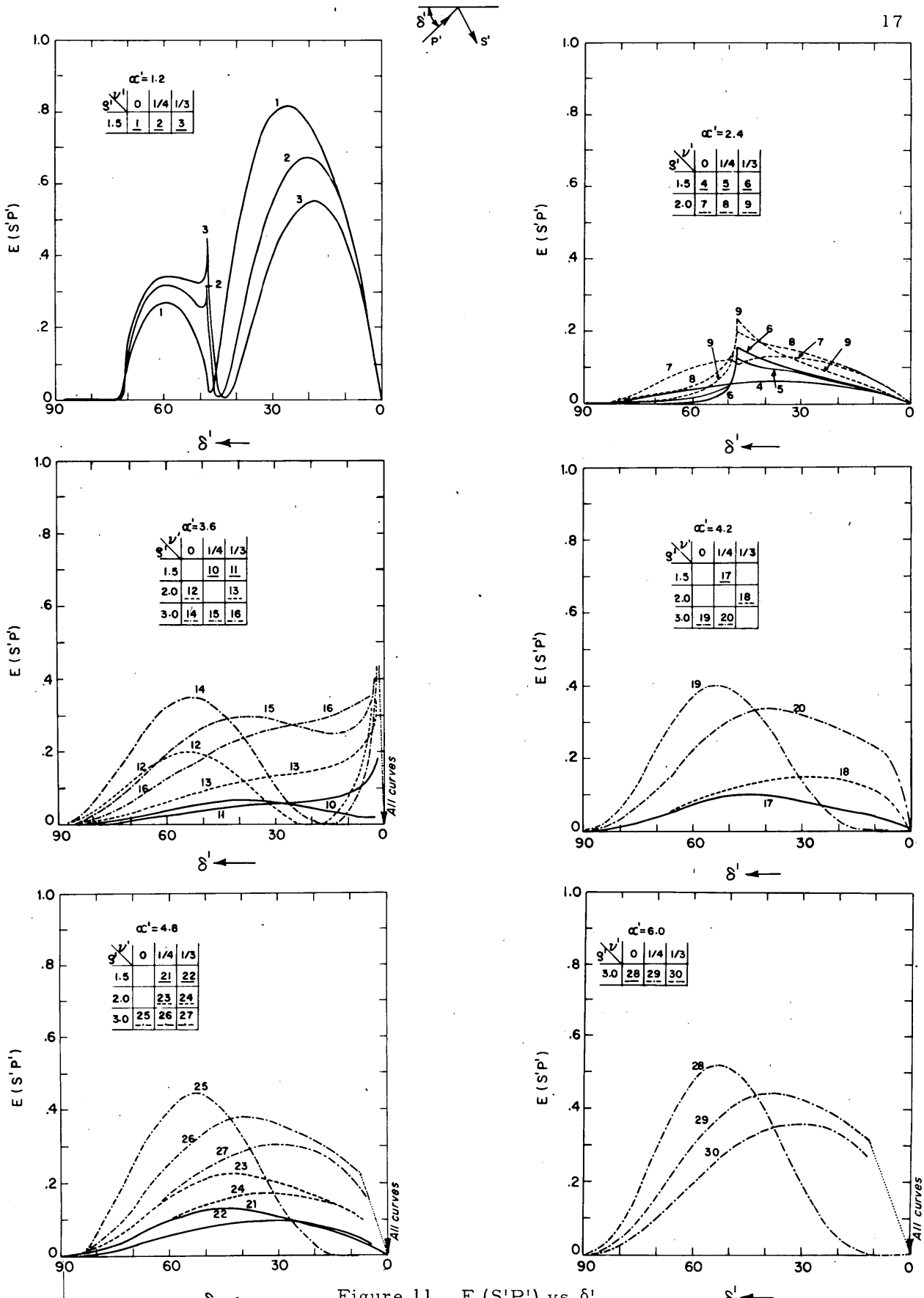


Figure 11. E (S'P') vs δ'